

## References

- GOEL, K. K., PRUCNAL, P. R., SHIMAZU, Y., MILBRODT, M., DESURVIRE, E., and TELL, B.: 'Demonstration of packet switching through an integrated-optic tree switch using photoconductive logic gates', *Electron. Lett.*, 1990, **26**, pp. 287-289
- HA, W. L., FORTENBERRY, R. M., and TUCKER, R. S.: 'Demonstration of photonic fast-packet switching at 700 Mb/s', *Electron. Lett.*, 1991, **27**, pp. 789-790
- MACE, D. A. H., ADAMS, M. J., SINGH, J., FISHER, M. A., and HENNING, I.: '1 × 2 lossless semiconductor optical switch', *Electron. Lett.*, 1991, **27**, pp. 198-199
- CAVANAGH, B., MARSHALL, I. W., SHERLOCK, G., and WICKES, H.: 'Comparison of bulk buried heterostructure and multiple quantum well laser amplifier switches', *Electron. Lett.*, 1991, **27**, pp. 263-265
- EVANKOW, J. D., JUN., and THOMPSON, R. A.: 'Photonic switching modules designed with laser diode amplifiers', *IEEE J. Sel. Areas Commun.*, 1988, **6**, pp. 1087-1095
- MINZER, S. E.: 'Broadband ISDN and asynchronous transfer mode (ATM)', *IEEE Commun. Mag.*, 1989, **27**, pp. 17-24
- FORTENBERRY, R. M., HA, W. L., and TUCKER, R. S.: 'Photonic fast packet switch with gain'. Tech. Dig. Topical Meeting on Photonic Switching, Salt Lake City, 1991, pp. 128-131

## CW ROOM TEMPERATURE UPCONVERSION LASING AT BLUE, GREEN AND RED WAVELENGTHS IN INFRARED-PUMPED Pr<sup>3+</sup>-DOPED FLUORIDE FIBRE

Indexing terms: Lasers, Optical fibres

Continuous-wave, room temperature laser oscillation at 491 nm, 520 nm, 605 nm and 635 nm in a Pr<sup>3+</sup>-doped fluorozirconate fibre pumped simultaneously at 1.01 μm and 0.835 μm is reported. An output power of 185 mW has been measured for the 635 nm transition. The thresholds obtained suggest that laser diode-pumped operation of all four transitions should be possible in an optimised fibre.

**Introduction:** There is currently a great deal of interest in the development of simple and compact sources of coherent visible radiation. Two promising techniques for the development of such sources are second harmonic generation, either directly of the output from laser diodes<sup>1</sup> or of the output from a laser diode-pumped laser,<sup>2</sup> and upconversion lasing where two or more photons from a pump source are absorbed by a single rare earth ion which subsequently emits a single higher energy photon. A variety of upconversion laser systems based on both multi-ion<sup>3</sup> and single ion<sup>4</sup> processes have been demonstrated. This technique has the advantage of simplicity, in that no stabilised resonant cavity is needed, but also the disadvantage that in most cases the efficiency of upconversion is found to be strongly temperature dependent so that cooling to liquid nitrogen (or lower) temperatures is required. However, Allain *et al.*<sup>5</sup> have recently demonstrated an efficient Ho<sup>3+</sup>-doped fluorozirconate fibre laser operating in the green at room temperature with red krypton laser pumping. This laser demonstrated the great benefit of using the fibre geometry where small core diameter allowed the high intensities required for efficient upconversion to be maintained over a long interaction length. Allain *et al.*<sup>6</sup> have also previously reported on Pr<sup>3+</sup>-doped fluorozirconate fibre lasers operating at orange and red wavelengths when pumped with an argon laser operating at 476.5 nm.

We report on Pr<sup>3+</sup>-doped fluorozirconate fibre lasers which are pumped in the infrared at 1.01 μm and 835 nm and lase in the blue (491 nm), green (520 nm), orange (605 nm) and red (635 nm) wavelength regions. The great attraction of pumping at infrared wavelengths is that high power laser diodes are available and so it may be possible to construct efficient, high power, all-solid-state blue green and red sources based on upconversion in Pr<sup>3+</sup>-doped fibres. Such sources may be expected to find applications in areas such as optical data storage, undersea communications and projection televisions.

**Experiment:** The fibre used for the experiments had a ZBLANP core doped with Pr<sup>3+</sup> ions at a concentration of 560 ppm (by weight) and a cladding of ZBLAN glass. The core diameter of the fibre was 4.6 μm and the numerical aperture 0.15 with a cutoff wavelength for the LP<sub>11</sub> mode of 0.9 μm. An energy level diagram for the Pr<sup>3+</sup> ion in a ZBLANP host glass is shown in Fig. 1. A Ti:sapphire laser tuned to 1.01 μm was used to excite Pr<sup>3+</sup> ions from the <sup>3</sup>H<sub>4</sub> ground state to the <sup>1</sup>G<sub>4</sub> multiplet. A second Ti:sapphire laser tuned to 835 nm

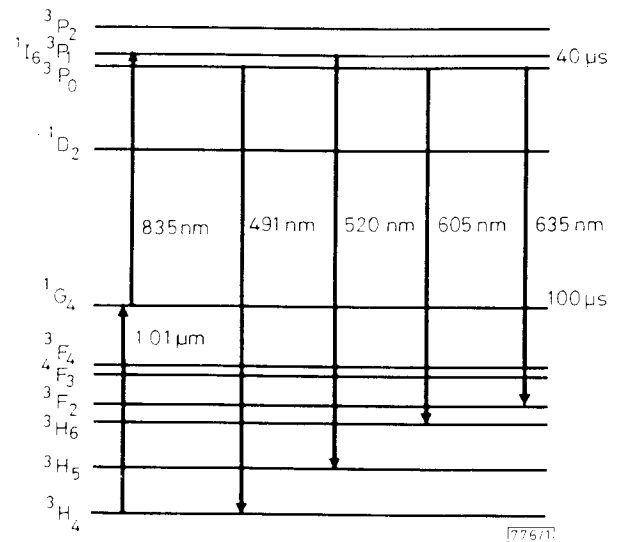


Fig. 1 Energy level diagram for Pr<sup>3+</sup>-doped ZBLANP glass showing pumping scheme and laser transitions

was used to provide excitation from the <sup>1</sup>G<sub>4</sub> multiplet to the thermally coupled <sup>3</sup>P<sub>1</sub>, <sup>1</sup>I<sub>6</sub> and <sup>3</sup>P<sub>0</sub> levels.

Initial experiments on the red laser transition were performed with a fibre length of approximately 10 m. Pump light from both Ti:sapphire lasers was combined using a polarisation rotator and beamsplitter. This light was launched co-propagating into the fibre by a ×20 microscope objective at an efficiency of ≈30-40% for each pump beam. At the launch end the fibre was butted against a dielectric mirror of >99% reflectivity from 600 nm to 640 nm and ≈80% transmission at both pump wavelengths. The laser cavity was completed by the ≈4% Fresnel reflection arising from the fibre/air interface. The pump power from the Ti:sapphire laser operating at 835 nm was set at 700 mW incident on the launch objective. The laser power at 635 nm (<sup>3</sup>P<sub>0</sub>-<sup>3</sup>F<sub>2</sub> transition) was then monitored as a function of the power from the Ti:sapphire laser operating at 1.01 μm and these results are shown in Fig. 2. The slope efficiency with respect to incident 1.01 μm pump power was ≈9.6%. The maximum power extracted from this laser was ≈185 mW. This data point was obtained by tuning the pump wavelength to 995 nm where 2 W of pump power was available and represents an overall power conversion efficiency of nearly 7% for infrared light to the red. The pump power was then set to 1 W at 1.01 μm and the red output power at 635 nm measured as a function of 835 nm pump power. This data set is also shown in Fig. 2. The slope efficiency with respect to incident 835 nm pump power was ≈14%. Some saturation of the 635 nm output power with respect to 835 nm pump power is evident. It is thought that this may possibly arise from the saturation of the 835 nm excited state absorption, although it may also be caused by the 835 nm pump beam moving (and hence launch efficiency changing) as the power was attenuated. Significant improvements to these results may be expected when using a fibre of lower background loss than the current value of 0.3 dB/m. Pr<sup>3+</sup>-doped ZBLAN fibres with losses of ≈0.1 dB/m have previously been fabricated.<sup>7</sup> The red transition at 635 nm was the only one on which laser oscillation could be obtained when using the 10 m length of fibre.

Because it was clear that by no means all of the 10 m length of fibre was significantly pumped further experiments were then performed on a fibre length of ≈1.2 m. With this length of fibre the 635 nm transition was below threshold unless added feedback was provided and so it was possible to investi-

gate other laser transitions. Using a cavity containing two mirrors of >99% reflectivity in the red butted against the

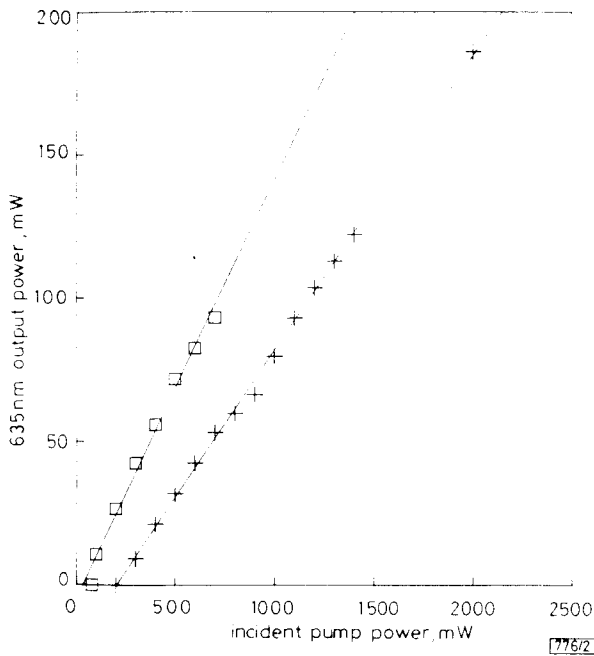


Fig. 2 Output power at 635 nm as function of pump power for  $\text{Pr}^{3+}$ -doped ZBLANP fibre laser

Fibre length  $\approx 10$  m  
 □ 1 W at 1.01  $\mu\text{m}$   
 Varying at 835 nm  
 + 700 mW at 835 nm  
 Varying at 1.01  $\mu\text{m}$

fibre, incident pump power thresholds as low as 40 mW at 1.01  $\mu\text{m}$  with 10 mW at 835 nm and 40 mW at 835 nm with 20 mW at 1.01  $\mu\text{m}$  were obtained. This fibre length is much shorter than the optimum because the ground state absorption at 1.01  $\mu\text{m}$  is <2 dB/m for this fibre and so a longer fibre length would allow more pump power to be absorbed.

The mirror at the output end of the cavity was then changed to one of  $\sim 40\%$  reflectivity at 605 nm and  $\sim 20\%$  reflectivity at 635 nm. With this cavity laser oscillation was observed at 605 nm on the  ${}^3\text{P}_0\text{-}{}^3\text{H}_6$  transition. The 1.01  $\mu\text{m}$  pump power was set to 1 W and the 605 nm output power measured as a function of the 835 nm output power and the results are shown in Fig. 3. For low values of 835 nm pump

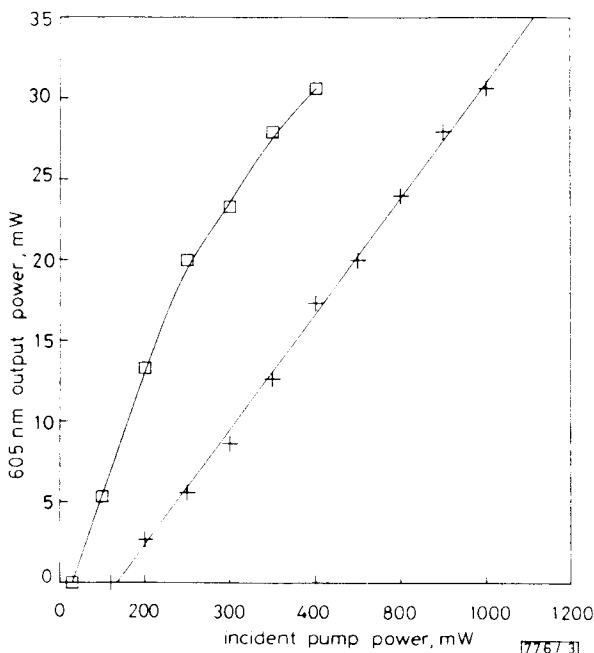


Fig. 3 Output power at 605 nm as function of pump power for  $\text{Pr}^{3+}$ -doped ZBLANP fibre laser

Fibre length  $\approx 1.7$  m  
 □ 1 W at 1.01  $\mu\text{m}$   
 Varying at 835 nm  
 + 1 W at 1.01  $\mu\text{m}$   
 Varying at 605 nm

power the slope efficiency is approximately 7% with respect to incident pump power. The saturation of the 605 nm output power with respect to 835 nm pump power is thought to arise from the saturation of the 835 nm excited state absorption. The maximum 605 nm power extracted was approximately 30 mW. An improved performance should be possible with a longer fibre length where there would be greater absorption at both pump wavelengths. The 835 nm power was then set to 600 mW and the 605 nm output power measured as a function of 1.01  $\mu\text{m}$  power. These results are also shown in Fig. 3, where the slope efficiency with respect to 1.01  $\mu\text{m}$  pump power is  $\sim 3.3\%$ .

Both mirrors were then changed to mirrors of >99% reflectivity in the green. With a cavity completed with these mirrors laser oscillation was observed at 520 nm on the  ${}^3\text{P}_1, {}^1\text{I}_6\text{-}{}^3\text{H}_5$  transition. A threshold of  $\sim 160$  mW of each pump wavelength was measured. Because the output coupling was <1%, the extracted output power was only of the order of 1 mW. For high pump powers simultaneous lasing in the green and red was observed. Clearly significant improvements in performance should be possible with a cavity using an optimised fibre length and an output coupler of higher transmission.

Laser oscillation has also been observed in the blue at 491 nm on the  ${}^3\text{P}_0\text{-}{}^3\text{H}_4$  three-level transition when completing the cavity with two high reflectors at this wavelength. The lowest threshold recorded was  $\sim 200$  mW of 835 nm pump power and 280 mW at 1.01  $\mu\text{m}$ . Again, the extracted powers were of the order of 1 mW because of the low transmission of the output coupler. For high pump powers simultaneous lasing at 635 nm occurred.

*Discussion:* We have demonstrated continuous-wave room temperature infrared-pumped upconversion lasers based on  $\text{Pr}^{3+}$ -doped fluorozirconate fibre which operate at blue, green, orange and red wavelengths. There is clearly plenty of scope for improving on the performance that we have obtained to date. By using a smaller core fibre with a cutoff wavelength of  $\sim 450$  nm it should be possible to reduce the pump powers required at each wavelength by up to a factor of four because the intensity scales inversely with the core area. This will reduce the threshold powers required for laser oscillation in the red to a level well within reach of that available from laser diodes. In addition to improvements resulting from the reduction in core diameter, further significant improvements should result from using a longer fibre length than the 1.2 m used for demonstrating laser oscillation in the blue, green and orange wavelength regions. Additionally, any pump light which was not absorbed in a single pass through the fibre could be fed back to be absorbed on a second pass. It is, therefore, not unreasonable to expect the thresholds for lasing on these transitions also to come down to a level available from semiconductor diode lasers. We believe that the results contained in this Letter represent a significant step towards the realisation of practical all-solid-state blue green and red upconversion lasers. Such devices have the attraction of cheapness and simplicity and could be expected to find numerous applications in a wide variety of fields.

R. G. SMART  
 D. C. HANNA  
 A. C. TROPPER

9th May 1991

Optoelectronics Research Centre  
 University of Southampton  
 Southampton SO9 5NH, United Kingdom

S. T. DAVEY  
 S. F. CARTER  
 D. SZEBESTA

British Telecom Research Laboratories  
 Martlesham Heath  
 Ipswich IP5 7RE, United Kingdom

## References

- 1 KOZLOVSKY, W. J., LENTH, W., LATTA, E. E., MOSER, A., and BONA, G. L.: 'Generation of 41 mW of blue radiation by frequency doubling of a GaAlAs diode laser', *Appl. Phys. Lett.*, 1990, **56**, pp. 2291-2292

2. RISK, W. P., PON, R., and LENTH, W.: 'Diode laser pumped blue-light source at 473 nm using intracavity frequency doubling of a 946 nm Nd : YAG laser', *Appl. Phys. Lett.*, 1989, **54**, pp. 1625-1627
3. HEBERT, T., WANNEMACHER, R., LENTH, W., and MACFARLANE, R. M.: 'Blue and green cw upconversion lasing in Er: YLiF<sub>4</sub>', *Appl. Phys. Lett.*, 1990, **57**, pp. 1727-1729
4. ALLAIN, J. Y., MONERIE, M., and POIGNANT, H.: 'Blue upconversion fluorozirconate fibre laser', *Electron. Lett.*, 1990, **26**, pp. 166-168
5. ALLAIN, J. Y., MONERIE, M., and POIGNANT, H.: 'Room temperature CW tunable green upconversion holmium fibre laser', *Electron. Lett.*, 1990, **26**, pp. 261-263
6. ALLAIN, J. Y., MONERIE, M., and POIGNANT, H.: 'Tunable CW lasing around 610, 635, 695, 715, 885 and 910 nm in praseodymium-doped fluorozirconate fibre', *Electron. Lett.*, 1991, **127**, pp. 189-191
7. CARTER, S. F., SZEBESTA, D., DAVEY, S. T., WYATT, R., BRIERLEY, M. C., and FRANCE, P. W.: 'Amplification at 1.3 μm in a Pr<sup>3+</sup>-doped single-mode fluorozirconate fibre', *Electron. Lett.*, 1991, **27**, pp. 628-629

## REACTANCE ANISOTROPY IN SUPERCONDUCTING YBa<sub>2</sub>Cu<sub>3</sub>O<sub>7-x</sub> FILMS

Indexing terms: Superconductors, Thin films

The reactance of thin epitaxial films of YBa<sub>2</sub>Cu<sub>3</sub>O<sub>7-x</sub> has been measured as a function of temperature, frequency and film crystallographic orientation. The films were grown on SrTiO<sub>3</sub> and MgO single crystal substrates by *in situ* RF sputter deposition. For YBa<sub>2</sub>Cu<sub>3</sub>O<sub>7-x</sub> deposited on SrTiO<sub>3</sub> (110) the film reactance is capacitive for temperatures between 300 K and  $T_c$  and frequencies above a few kilohertz. Below  $T_c$  the reactance of the films is inductive. For  $T > T_c$  the (resonant) frequency at which  $X = 0$  decreases for increasing temperatures and the films are inductive for frequencies less than the resonant frequency. For well orientated films deposited onto SrTiO<sub>3</sub> (100) and MgO (100) substrates the reactance is purely inductive for temperatures between 10-300 K and frequencies up to 13 MHz.

**Introduction:** The electrical properties of high  $T_c$  materials can be highly anisotropic.<sup>1</sup> This arises from the anisotropic unit cell structure which has a conducting Cu-O layer in the *ab* plane separated by insulating layers in the *c* direction.<sup>2</sup> The electrical resistivity in the Cu-O *ab* plane is metallic-like whereas the resistivity in the *c* direction has semiconductor characteristics and charge transport occurs by tunnelling between the Cu-O planes.<sup>3</sup> A large anisotropy difference in the reactance is also expected but this does not appear to have been reported yet. If the driving field is sinusoidal the material impedance is  $Z = R_n + jX$  where  $R_n$  is the normal resistance which is zero in the steady state.  $X$  is the sum of the inertial reactance of the normal carriers and super carriers. In the *ab* Cu-O plane we expect this to be purely inductive because of the metallic nature of these planes. However, for transport in the *c* direction across the Cu-O planes a capacitive displacement current may be expected. Hence the reactance may be positive or negative depending on the crystal orientation. We report measurements of the anisotropic reactance and its temperature and frequency dependence for epitaxially grown thin films of YBa<sub>2</sub>Cu<sub>3</sub>O<sub>7-x</sub> RF sputtered on SrTiO<sub>3</sub> and MgO single crystal substrates.

**Experimental techniques:** The superconducting YBa<sub>2</sub>Cu<sub>3</sub>O<sub>7-x</sub> films were produced *in situ* by RF magnetron sputtering using a single compound YBa<sub>2</sub>Cu<sub>3</sub>O<sub>7-x</sub> target 52 mm in diameter. The substrates and heater were mounted perpendicular to the sputtered vapour diffusion front and at an angle of about 56° to the target surface. The temperature of the heater was measured with a chromel-alumel (Cr/Al) (type K) thermocouple spot welded to the heater close to the substrates. Silver foil was placed between the substrates and heater plate to improve thermal contact. In the experiments reported here the substrate-temperature during deposition was 735°C, the argon/oxygen ratio 4:1 and the total gas pressure 280 mtorr.

The films were rapidly cooled in the oxygen ambient immediately after deposition. The films were very smooth glossy black/brown, highly adherent and superconducting as deposited. Electrical contacts to the films were made via four evaporated silver contacts. The samples were mounted onto a copper block in a closed cycle helium cryostat (Bio-Rad). Temperatures were measured using a calibrated silicon diode sensor and a 100 Ω platinum resistance sensor. Short wires (about 10 cm long) were connected to BNC connectors and bonded to the silver pads using silver paint. The AC measurements were obtained using an HP4192A impedance analyser operated in the series L, R mode. This was connected to BNC connectors on the cryostat via an HP four wire cable set calibrated to the analyser. Sample resistivity (or conductivity) may be obtained from  $\rho = RA/l$  where  $l = 1$  mm,  $A = wt$  where  $w = 5$  mm and  $t$  is the film thickness given in the Figures. The impedance analyser and electrometer were on line to a computer via an IEEE 488 bus for data collection and analysis. The structure of the films was analysed by x-ray diffraction and reflection high energy electron diffraction (RHEED). The YBa<sub>2</sub>Cu<sub>3</sub>O<sub>7-x</sub> films deposited onto SrTiO<sub>3</sub> (110) were (013) orientated and films on SrTiO<sub>3</sub> (100) or MgO (100) were (100) orientated. The critical current densities measured using the four-terminal method at 10 K for SrTiO<sub>3</sub> (110) and MgO (100) substrates were approximately  $1.3 \times 10^6$  A cm<sup>-2</sup> and  $5 \times 10^5$  A cm<sup>-2</sup>, respectively.

**Results and discussion:** The temperature dependence of resistance and reactance for a typical film deposited on SrTiO<sub>3</sub> (110) is shown in Fig. 1. Above  $T_c$  the reactance is negative and capacitive at 13 MHz. Below  $T_c$  the reactance is purely inductive. The variation of reactance with frequency for YBa<sub>2</sub>Cu<sub>3</sub>O<sub>7-x</sub> sputtered on SrTiO<sub>3</sub> (110) is presented in Fig. 2. For  $T < T_c$  the reactance is positive and inductive. In the

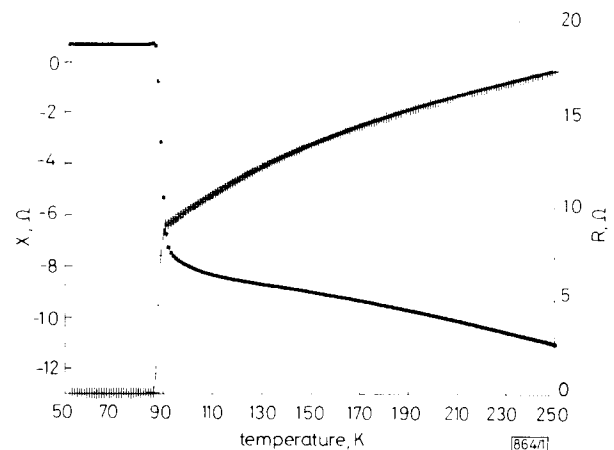


Fig. 1 Series resistance and reactance against temperature

YBa<sub>2</sub>Cu<sub>3</sub>O<sub>7-x</sub> RF sputtered on SrTiO<sub>3</sub> (110)

$t = 68$  nm

—□—  $X$   
—|—  $R$

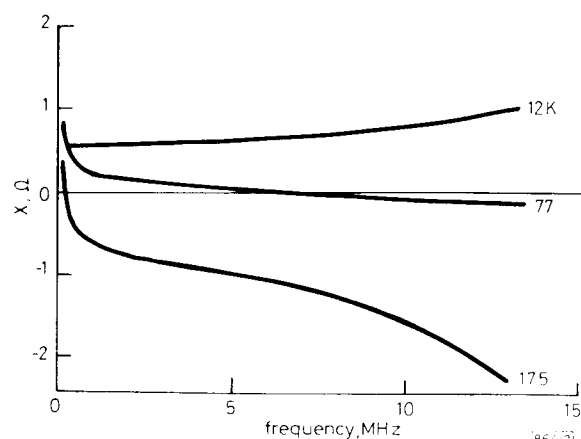


Fig. 2 Variation of reactance with frequency

YBa<sub>2</sub>Cu<sub>3</sub>O<sub>7-x</sub> RF sputtered on SrTiO<sub>3</sub> (110)

$t = 1300$  nm